JOURNAL OF VIROLOGY, Apr. 1998, p. 3278–3288 Vol. 72, No. 4
0022-538X/98/$04.00+0

Intracellular Complexes of Viral Spike and Cellular Receptor Accumulate during Cytopathic Murine Coronavirus Infections

PASUPULETI V. RAO AND THOMAS M. GALLAGHER*

Department of Microbiology and Immunology, Loyola University Medical Center, Maywood, Illinois 60153

Received 10 September 1997/Accepted 22 December 1997

Murine hepatitis virus (MHV) infections exhibit remarkable variability in cytopathology, ranging from acutely cytolytic to essentially asymptomatic levels. In this report, we assess the role of the MHV receptor (MHVR) in controlling this variable virus-induced cytopathology. We developed human (HeLa) cell lines in which the MHVR was produced in a regulated fashion by placing MHVR cDNA under the control of an inducible promoter. Depending on the extent of induction, MHVR levels ranged from less than ~1,500 molecules per cell (designated R^{lo}) to ~300,000 molecules per cell (designated R^{hi}). Throughout this range, the otherwise MHV-resistant HeLa cells were rendered susceptible to infection. However, infection in the R^{lo} cells occurred without any overt evidence of cytopathology, while the corresponding R^{hi} cells died within 14 h after infection. When the HeLa-MHVR cells were infected with vaccinia virus recombinants encoding MHV spike (S) proteins, the R^{hi} cells succumbed within 12 h postinfection; R^{lo} cells infected in parallel were intact, as judged by trypan blue exclusion. This acute cytopathology was not due solely to syncytium formation between the cells producing S and MHVR, because fusion-blocking antiviral antibodies did not prevent it. These findings raised the possibility of an intracellular interaction between S and MHVR in the acute cell death. Indeed, we identified intracellular complexes of S and MHVR via coimmunoprecipitation of endoglycosidase H-sensitive forms of the two proteins. We suggest that MHV infections can become acutely cytopathic once these intracellular complexes rise above a critical threshold level.

Virus persistence requires that infection occur with little or no cytolysis (1). Such asymptomatic infections may be a stable feature of the virus-host interaction (e.g., arenavirus infections [7]), or they may alternatively arise during a cytopathic infection by changes that reduce cytolytic potential (e.g., reovirus infections [18]). In vitro and in vivo infections by murine hepatitis virus (MHV) can readily shift from acutely cytolytic to persistent asymptomatic phases (6, 37, 49, 54). Thus, genetic and biochemical determinants of cytolytic potential can be revealed through studies of MHV infections.

Determinants of lytic potential can be categorized into virus-encoded and cell-encoded groups. With respect to the viral determinants, numerous correlations between changes in MHV genome sequence and MHV-induced cytopathology have been made (22, 32, 33, 56). These studies were tenable for two reasons; first, the 32-kb RNA genome of MHV is subject to spontaneous mutation (41); second, such mutants can be isolated, sequenced, and assessed for pathogenic potential. Most mutations correlating with changes in virus-induced pathology localize to the 4.1-kb open reading frame encoding the major surface (S) glycoprotein of the virus.

Current understanding of the biological functions of the S protein supports the contention that changes in this viral protein might affect the pathology of infection. The S protein forms the most prominent projections of the coronavirus particle (16). These projections are essential for delivery of the MHV genome into cells. They bind to cellular receptors (12, 27), and they additionally carry out the virion-cell membrane fusion event that occurs subsequent to receptor binding (55). Finally, there is definitive evidence from expression of mutated cDNAs that changes in S structure will alter its receptor binding and membrane fusion properties (28, 29), and these changes are indeed correlated with profound changes in virus-induced cytopathology (14, 22).

Cellular determinants of lytic potential appear somewhat varied and are best understood in the context of S-protein function. For example, the lipid composition of cellular membranes impacts MHV-induced cytopathology (17, 47). This is not surprising in light of our understanding that S proteins become cytopathic as they accumulate on the surface of infected cells and begin to mediate intercellular fusion (12). However, this fusion (and hence cytopathic effect) is generally inhibited by increases in the unsaturated fatty acid content of membranes (9, 47). The protease content of host cells also impacts MHV-induced cytopathology (23). Mechanistic explanations of this finding appeal to S-protein structure and function; S proteins undergo a proteolytic cleavage event during exocytosis through the Golgi apparatus, and oligomers comprised of the cleaved S products (S1 and S2) induce cytopathic membrane fusion more effectively than their uncleaved precursors (53).

Cellular receptors for MHV play an obvious role in virus-induced cytopathology. The primary receptor (termed MHVR [21]) molecules are required to initiate infection as they are specifically recognized by the S proteins protruding from the virion membrane (19, 20). MHVR also promotes expansion of infection between cells, as S proteins on infected cells bind to MHVR on neighboring cells, thereby promoting syncytia. Recent studies of tissue culture cells persistently infected with MHV reveal relatively few virus-induced syncytia and, at the same time, relatively low levels of MHVR (11, 48). Thus, it is conceivable that reduced levels of MHVR on cells might be responsible for reduced virus-induced cytopathology, but such a hypothetical relationship is far from clear as no defined culture has been developed in which MHVR levels could be adjusted.

Thus, we developed a set of HeLa cell-MHVR transfectants

* Corresponding author. Mailing address: Department of Microbiology and Immunology, Loyola University Medical Center, 2160 S. First Ave., Maywood, IL 60153. Phone: (708) 216-4850. Fax: (708) 216-9574. E-mail: tgallag@luc.edu.

that vary only in their levels of intracellular and surface MHVR. Using these cell lines, we found that the MHVR densities required for infection by virions were in fact lower than those that promote development of syncytia. With these cell lines, we made the additional observation that virus-induced cytopathology increases with increasing receptor levels. We found that the S protein, when produced in the absence of the other coronavirus proteins, will rapidly kill only those HeLa cells that produce abundant MHVR. Furthermore, we found that this cell death does not require the formation of syncytia; the death in fact occurs in well-separated cells and thus may arise by formation of S-MHVR complexes within intracellular organelles.

MATERIALS AND METHODS

Cells and viruses. HeLa-tTA (tTA denotes tetracycline-controlled transactivator) (35), HeLa-MHVR (29), and rabbit kidney clone 13 (RK13) cells were grown in Dulbecco's modified Eagle's medium (DMEM) supplemented with 10% heat-inactivated fetal bovine serum (ΔFBS) (Gibco-BRL Corp.). EBNA-sMHVR-Ig (28) cells were grown in DMEM–10% ΔFBS containing the antibiotics G418 (100 μg/ml) and hygromycin B (200 μg/ml). Murine 17 cl 1 cells (51) were grown in DMEM containing 5% tryptose phosphate broth (Difco Laboratories) and 5% ΔFBS. MHV strain A59 (MHV-A59) was grown in 17 cl 1 culture, and virions were purified as previously described (29). Infectivities of MHV-A59 were determined by plaque assay, using HeLa-MHVR (line 5) as indicator cells. Recombinant vaccinia viruses were grown and titered in RK13 cell cultures.

Quantitation of MHVR levels following doxycycline exposure. To alter MHVR levels, doxycycline (Sigma Co.) was added to the growth medium above HeLa-MHVR (line 5) cells at concentrations from 10^{-3} to 10^{0} μg/ml for various time periods. Cell surface MHVR levels were then measured by fluorescence-activated cell sorting (FACS). To this end, approximately 10^6 cells were incubated with 5 μl of monoclonal antibody (MAb) CC1 (58) in a volume of 250 μl of phosphate-buffered saline (PBS)–2% bovine serum albumin (BSA) for 30 min on ice. Cells were then pelleted, and unbound CC1 was removed by three cycles of resuspension and repelleting in ice-cold PBS. Rinsed cell pellets were resuspended in 100 μl of PBS–2% BSA containing 1 μl of fluorescein isothiocyanate (FITC)-conjugated goat anti-mouse immunoglobulin G (IgG) antibody (Cappell, Inc.). After 30 min on ice, unbound antibody was removed and the final pellets were suspended in 1 ml of PBS. Fluorescence profiles were obtained using a FACStar Plus (Becton Dickinson Co.), and the calculated mean fluorescence intensities (MFI) were taken as indicators of the cell surface MHVR levels.

Quantitation of MHVR levels by immunoblot analysis. HeLa-tTA or HeLa-MHVR cells (10^8) were dissolved in 1 ml of radioimmunoprecipitation assay (RIPA) buffer (10 mM Tris-HCl [pH 7.2], 150 mM NaCl, 1% sodium deoxycholate, 0.1% sodium dodecyl sulfate [SDS], 1% Triton X-100). Serial dilutions were prepared with RIPA buffer as diluent, and each sample (10 μl) was mixed with 20 ng of sMHVR-Ig (28), which served as an internal quantitation standard. These samples were then electrophoresed on SDS-polyacrylamide gels (40) and transferred to nitrocellulose filters. Authentic MHVR (110 kDa) and sMHVR-Ig (48 kDa) were identified on the filters by primary incubation with MAb CC1 (0.1%) in binding buffer (PBS–3% BSA–0.1% Tween 20) for 2 h at 22°C. Filters were then incubated with 0.1% goat anti-mouse Ig-alkaline phosphatase conjugate (Cappell) in binding buffer for 2 h at 22°C. Immobilized alkaline phosphatase was enzymatically detected with 5-bromo-4-chloro-3-indolylphosphate–toluidinium nitroblue tetrazolium reagent (Pierce Co).

Indirect immunofluorescence. Adherent HeLa-MHVR cells were grown on glass coverslips and then infected with MHV-A59 at various multiplicities. At 8 or 12 h postinfection, the cells were washed with PBS and then fixed alternatively in acetone or in PBS–3.7% formaldehyde. Formaldehyde-fixed cells were permeabilized for 10 min in PBS–0.1% Triton X-100. After rinsing with PBS, cells were incubated for 1 h at 22°C in PBS–2% BSA containing a 1:250 dilution of antimatrix MAb 5A5.2 (12). The bound MAb was detected with FITC-conjugated goat anti-mouse IgG antibody (1:1,000 in PBS–2% BSA), and cells were photographed with a Leitz fluorescence microscope.

Quantitative intercellular fusion assay. The cell fusion-dependent reporter gene (β-galactosidase) activation assay of Nussbaum et al. (45) was performed as described earlier (46), with minor modifications. Briefly, HeLa-MHVR^{lo} cells were coinfected with MHV-A59 and with vaccinia virus strain WR, each at a multiplicity of infection (MOI) of 10 PFU/cell. After 1 h, these cells were further transfected by lipofection with the reporter gene construct pGINT7β-gal (kindly provided by Richard A. Morgan, National Center for Human Genome Research, Bethesda, Md.). Five hours later, the cells were overlaid onto confluent 5-cm^2 monolayers of HeLa (or HeLa-MHVR) cells that had been inoculated 12 h earlier with recombinant vaccinia virus vP11 (2). At hourly intervals thereafter, the mixed monolayers were lysed by addition of 0.5% Nonidet P-40 (NP-40) in PBS and the quantity of β-galactosidase was calculated as described earlier (46).

Single-cell lysis. Trypan blue exclusion was used as an indicator of cell viabilities. The measurements were made on subconfluent HeLa-MHVR cell monolayers (10^4 cells/cm^2) that were infected as described in the text. In all experiments, rabbit anti-A59 serum MK15 (kindly provided by Susan Baker, Loyola University Medical Center) was added at 3 h postinfection, to a final concentration of 1%. This addition prevented the syncytium formation that might otherwise occur to a limited extent by ~8 h postinfection. Quantitations were performed at 14 h postinfection by trypsinizing adherent cells and suspending them along with the nonadherent populations into DMEM–10% ΔFBS. Cells were pelleted, resuspended in PBS–0.2% trypan blue (Gibco BRL), and counted. Each experimental condition was assayed in triplicate, and a minimum of 150 total cells were counted in each condition.

Electron microscopy. Transmission electron microscopic studies were done on HeLa-MHVR cell monolayers (10^4 cells/cm^2) that were infected with MHV-A59 (10 PFU/cell). At 10 h postinfection, monolayers were fixed in PBS containing 4% glutaraldehyde for 2 h at 4°C, then scraped from the dishes with a rubber policeman, pelleted by centrifugation, and washed with PBS by resuspension and repelleting. The final cell pellets were postfixed in PBS containing 1% osmium tetroxide for 1 h at 22°C and then treated with 0.1 M sodium cacodylate (pH 7.4) containing 1% tannic acid for 0.5 h at 22°C. Cells were repelleted, dehydrated in acetone, and embedded in Embed 812 (EM Sciences, Inc.). Sections of 70 nm were prepared on copper grids and stained for 10 min at 22°C with 5% uranyl acetate and then with Reynold's lead citrate for 5 min at 22°C. Sections were examined in a Hitachi H-600 electron microscope (70 kV).

Coimmunoprecipitation of S protein-MHVR protein complexes. To allow for the synthesis of the S protein within cells producing MHVR, HeLa-MHVR monolayers (10^6 cells/10 cm^2) were coinfected with vTF7.3 (26) and vTM1-S_{JHM} (32) for 1 h at 2 PFU/cell. Where indicated, infected cells were radiolabeled with [^{35}S]methionine (Tran^{35}S-label; ICN Pharmaceuticals, Inc.) from 3 to 7 h postinfection. Cell lysis was then achieved by using PBS–0.5% NP-40 at 22°C. Nuclei were removed by centrifugation, and cytoplasmic extracts (0.5 ml/10^6 cells) were mixed with 5 μl of rabbit antipeptide serum 874 (kindly provided by Michael J. Buchmeier, Scripps Research Institute) and with 10 μl of 50% (vol/vol) Sepharose-protein G beads (Pharmacia Biotech). After a 2-h incubation at 4°C, beads were washed by sequential resuspension and repelleting, using first ice-cold buffer A (0.01 M Tris-HCl [pH 7.2], 1 M NaCl, 0.1% NP-40), then buffer B (0.01 M Tris-HCl [pH 7.2], 0.1 M NaCl, 0.3% SDS, 0.1% NP-40, 0.001 M EDTA), and then buffer C (0.01 M Tris-HCl [pH 7.2], 0.1% NP-40). Where indicated, the final bead pellets were resuspended in endoglycosidase H buffer (0.05 M sodium phosphate [pH 6.5], 0.1% SDS, 1 mM phenylmethylsulfonyl fluoride). Samples in the endoglycosidase H buffer were incubated for 4 h at 37°C in the presence of 0.5 mU of endoglycosidase H (Boehringer Mannheim). Radiolabeled proteins were removed from the beads by addition of sample solubilizer (40) and a 5-min incubation at 100°C. Proteins were separated on SDS-polyacrylamide gels, impregnated with Entensify reagent (DuPont Corp.), and visualized by fluorography.

RESULTS

Regulated production of MHVR. Preliminary studies of a series of HeLa-MHVR transfectants that we developed in our laboratory (29) indicated that they varied substantially in MHVR production levels. Each cell line also varied in its capacity to serve as an indicator of MHV-A59 infectivity. In some transfectant lines, MHV-A59 produced large clear plaques; in others, only small pinprick plaques were observed. These basic observations suggested that MHVR levels influence MHV-A59 infection and syncytium formation.

To further explore the role of the MHVR in controlling virus infection characteristics, we set out to adjust MHVR levels over a wide range in an individual HeLa-MHVR line (line 5). This was possible because our stably transfected cells contained the MHVR cDNA under the control of an inducible transcription apparatus (35). In this system, cDNA transcription was dependent on the binding of a tTA protein to operator DNA sequences; addition of tetracycline to growth medium would cause the release of the tTA protein from operator DNA and thus would effect a decline in transcription (Fig. 1).

Transfectant line 5 was incubated in the presence of the tetracycline-derivative doxycycline (34) at 1 μg/ml, and the levels of MHVR on the cell surface were detected by incubation with antireceptor MAb CC1 (58) and FACS analyses. Initial results from these experiments indicated that lengthy incubation periods with doxycycline were necessary for establishment of new steady-state MHVR levels (Fig. 2). In the presence of doxycycline, MHVR levels decreased 10-fold after 4 days and continued to decrease thereafter, reaching a mini-

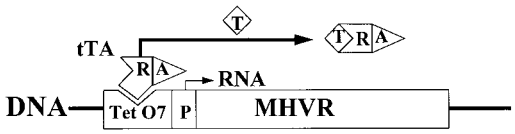

FIG. 1. Schematic depiction of the tetracycline-controlled expression system. tTA is a constitutively synthesized recombinant protein containing separate domains for transcriptional activation (A) and for DNA binding (R). Addition of tetracycline (T) to culture medium releases the tTA from operator DNA (TetO7), thereby preventing transcription of MHVR cDNA from the minimal cytomegalovirus promoter (P).

mum level after 7 days (Fig. 2A). When these cultures containing minimal levels of MHVR were shifted to media lacking doxycycline, a return to high MHVR levels was observed, but the increases began only after a 3-day delay period (Fig. 2B).

To obtain transfectant cells with unique steady-state MHVR levels, parallel cultures of line 5 were incubated for a week in graded doses of doxycycline ranging from 10^{-3} to 10^{0} μg/ml. Assays for surface MHVR levels in these cultures were then performed by FACS as described above. The results (Fig. 3) revealed that the doxycycline treatments yielded a series of HeLa cultures that we contend vary only in the amount of MHVR that they produce. Cells with the highest receptor levels (MFI of 1,100) were designated R^{hi} (Fig. 3A), those with intermediate levels (MFI of 56) were designated R^{int} (Fig. 3D), and those with the lowest levels (MFI of 8) were designated R^{lo} (Fig. 3E).

To determine the relationship between the MFI values obtained by FACS analysis and the actual number of MHVR molecules present in the HeLa transfectants, we performed an immunoblotting procedure that allowed us to compare the amount of MHVR in cell lysates with a known quantity of soluble recombinant MHVR (termed sMHVR-Ig [28]). To this end, we prepared lysates of R^{hi} and R^{lo} cells and then subjected the proteins in each lysate to SDS-polyacrylamide gel electrophoresis in conjunction with 20 ng of sMHVR-Ig. After transfer of the proteins to nitrocellulose, antireceptor MAb CC1 was used to identify the 110-kDa authentic MHVR and the 48-kDa sMHVR-Ig. The results (Fig. 4) indicated that 3×10^5 R^{hi} cells contained an amount of receptor roughly equivalent to 20 ng of the internal sMHVR-Ig standard; this corresponds to ~300,000 receptors per cell. Immunoblot signals

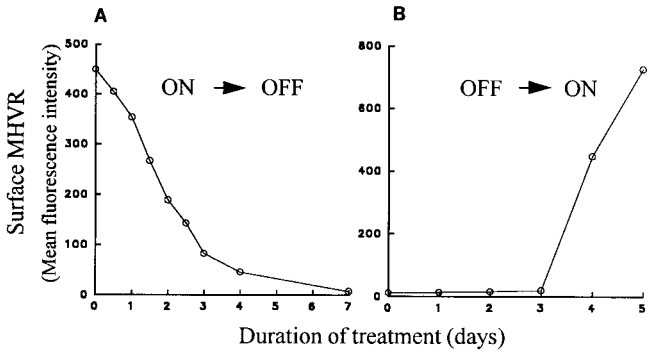

FIG. 2. Time required for doxycycline to change surface MHVR levels. Stably transfected HeLa-MHVR cells (line 5) were incubated in DMEM–10% ΔFBS, either with or without doxycycline, and the cell surface MHVR levels were measured by flow cytometric analysis. The mean of fluorescence intensity for each sample was calculated and plotted after subtraction of background (HeLa-tTA cell) fluorescence. (A) Addition of 1 μg of doxycycline per ml at time zero; (B) removal of doxycycline at time zero from cultures exposed for the prior 2 weeks in 1 μg of doxycycline per ml.

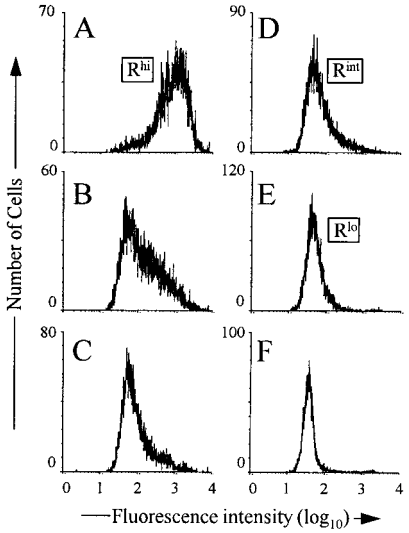

FIG. 3. FACS profiles of HeLa-MHVR cells treated with graded doses of doxycycline. Cells were incubated in DMEM–10% ΔFBS containing 0 (A), 0.001 (B), 0.01 (C), 0.1 (D), and 1 (E) μg of doxycycline per ml for 2 weeks at 37°C. Cell surface MHVR levels were measured as described in Materials and Methods. (F) FACS profiles of untransfected HeLa-tTA cells.

were not detected among proteins from 2×10^6 R^{lo} cells (Fig. 4, rightmost lane); our detection limit in this assay was ~1,500 receptors per cell. Our immunoblot and FACS data were generally consistent with each other. The FACS-derived MFI values for the R^{lo} cells were 140 times lower than those for R^{hi} cells, suggesting an average of ~300,000/140, or ~2,000 receptors per R^{lo} cell.

Comparisons of the R^{lo} and R^{hi} cells following murine coronavirus infection. (i) Both R^{lo} and R^{hi} cells can be infected. The cultures, which varied only in the intracellular and cell surface density of MHVR, provided us with the opportunity to directly assess the role of receptor abundance in virion infection and syncytium formation. To assess this infection susceptibility, we challenged the cultures with MHV-A59, and at 8 h postinfection we identified cells producing the viral matrix protein by indirect immunofluorescence. We found that all the MHVR cultures, from R^{hi} to R^{lo}, contained matrix-positive (MHV-A59-infected) cells (Fig. 5). As expected, the proportion of infected cells increased with increasing MHVR levels, from 4% for R^{lo} to 62% for R^{hi}, at an MOI of 1 PFU/cell. These variations in infection susceptibility could not be attributed to the doxycycline used to modulate receptor levels be-

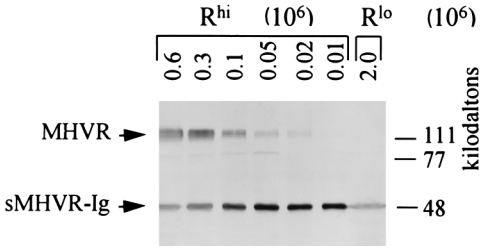

FIG. 4. Quantitation of MHVR content of R^{hi} and R^{lo} cells by Western immunoblotting. The HeLa-MHVR cells were solubilized with detergent-containing RIPA buffer, and the indicated cell equivalents were mixed with 20 ng of sMHVR-Ig (28) prior to electrophoresis and transfer to nitrocellulose. Immobilized MHVR was identified using antireceptor MAb CC1 (58) and alkaline phosphatase-conjugated second antibody as described in Materials and Methods.

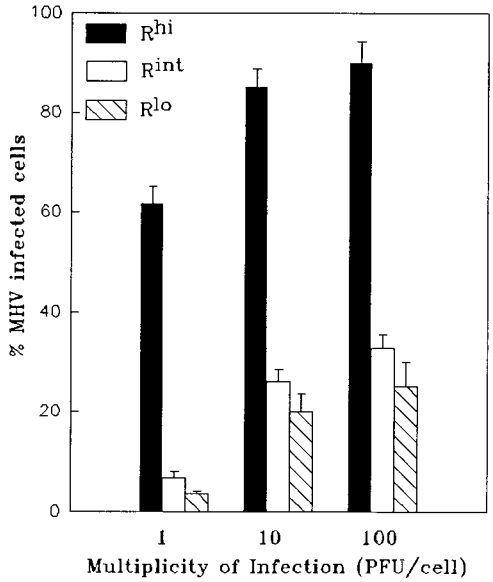

FIG. 5. Quantitation of infected HeLa-MHVR cells following challenge with MHV-A59. HeLa-MHVR cells were infected with MHV-A59 at the indicated multiplicities and 8 h later fixed in acetone and stained for the presence of the viral matrix protein by the immunofluorescence procedure described in Materials and Methods. The percentages of matrix-positive cells were calculated by counting at least 250 total cells for each experimental condition. Error bars represent standard deviations from the mean of three independent determinations.

cause the same doxycycline administrations to murine 17 cl 1 cultures did not alter either the number of A59-infected cells or the progeny virus yields (data not shown).

Inoculation at high input multiplicities increased the proportion of infected R^{lo} cells, but even at an input of 100 PFU/cell, only 28% of R^{lo} cells were infected (Fig. 5). According to the FACS profiles of antireceptor antibody-stained cells (Fig. 3), 28% of the $MHVR^{lo}$ cells had surface fluorescence levels greater than 17 MFI, which we contend corresponds to ~4,000 molecules of MHVR per cell. Thus, we conclude that MHVR levels must exceed ~4,000 per cell to become infected by MHV-A59 in our experiments.

(ii) The R^{lo} cells are resistant to virus-induced syncytium formation. Microscopic examination of immunostained R^{lo} monolayers at 14 h after A59 infection (100 PFU/cell) revealed the complete absence of virus-induced syncytia. R^{hi} cells infected in parallel were fused into a single unbroken syncytium (Fig. 6A and B). Similar observations were made in cultures inoculated at the lower input multiplicities of 1 and 10 PFU/cell (data not shown). That R^{lo} cells were sensitive to virion infection but resistant to syncytium formation suggested that virion entry required less cell surface MHVR than that required to promote intercellular fusion and thus warranted a closer examination. Therefore we quantitated the effect of MHVR levels on the promotion of virus-induced intercellular fusion by using a previously developed assay of cytoplasmic mixing (45, 46). The assay involved the introduction of the transcriptionally silent T7-βgal reporter plasmid into a population of A59-infected R^{lo} cells. After the display of the S protein on the plasma membrane, these cells were overlaid onto monolayers of R^{lo} or R^{hi} cells previously infected with vP11 (2), which encodes T7 RNA polymerase. Intercellular fusion resulting from the S-MHVR interaction would then cause cytoplasmic mixing and subsequent transcription of the β-galactosidase gene by the T7 polymerase.

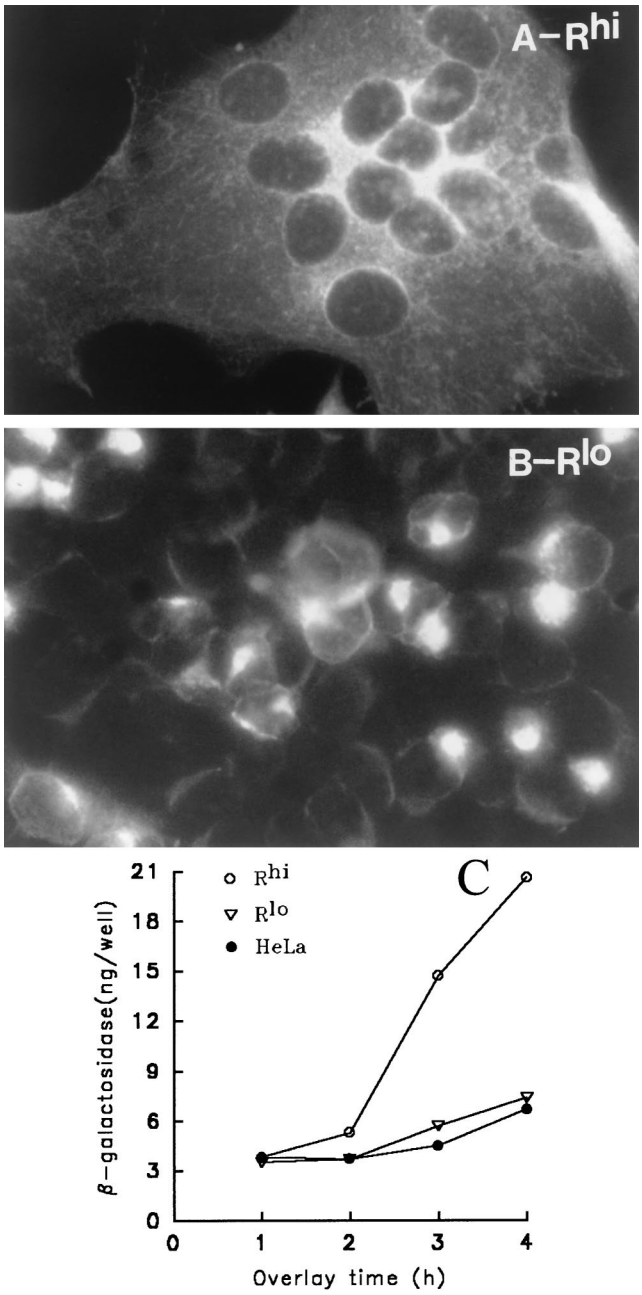

FIG. 6. Measurement of syncytia in MHV-A59-infected R^{hi} and R^{lo} cells. (A and B) Cells were processed as described in the legend to Fig. 5 at 8 h after MHV-A59 infection (MOI = 100 PFU/cell) and photographed with a Leitz fluorescence microscope. (C) The indicated cell monolayers were infected with vaccinia virus recombinant vP11, which causes T7 RNA polymerase to accumulate within the cells; 12 h later, these monolayers were overlaid with cells from a separate R^{lo} culture that was infected/transfected 5 h earlier with MHV-A59, vaccinia virus strain WR, and the β-galactosidase-encoding plasmid pT7-β-gal (45). These cells contain S protein on plasma membranes and transcriptionally silent β-galactosidase genes in cytosol. At hourly intervals following the overlay, cultures were lysed in PBS–0.5% NP-40 (5×10^5 cells/ml/well), and the quantities of β-galactosidase were determined by an enzymatic assay.

The results of β-galactosidase quantitation in the mixed cell monolayers (Fig. 6C) confirmed that the amount of receptor on the R^{lo} cell surface is not sufficient to promote any S-induced plasma membrane fusion. Increases in β-galactosidase activity following the mixing of A59-infected cells and R^{lo} cells

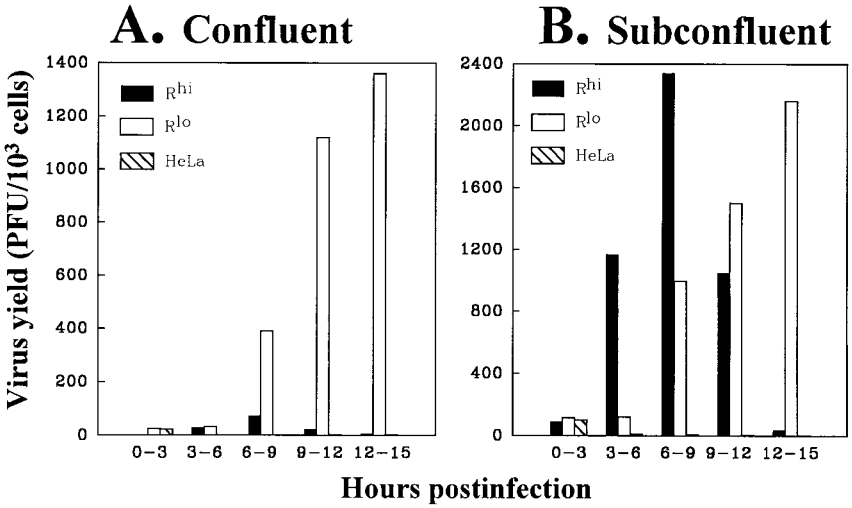

FIG. 7. Yields of MHV-A59 secreted from infected R^{hi} and R^{lo} cells. Following inoculation with MHV-A59 (MOI = 10 PFU/cell), cultures were incubated in DMEM–10% ΔFBS (1 ml/10^6 cells). At 3 h intervals, the DMEM–10% ΔFBS was removed and replaced with fresh medium. Viral infectivities in the spent media were determined by plaque assays using HeLa-$MHVR^{hi}$ cells as indicators.

were no different than parallel β-galactosidase increases following control mixing with receptor-negative HeLa-tTA cells. In contrast, A59-infected cells did fuse with the R^{hi} cells and consistently promoted β-galactosidase production that was three times the background levels.

We additionally found that this receptor-mediated enhancement of virus-induced syncytia extended to MHV strain JHM, a virus known to exhibit a syncytium-forming capacity so potent that it fuses even receptor-negative cells (31, 44). In parallel cytoplasmic mixing assays in which JHM replaced A59, we indeed observed a limited amount of receptor-independent fusion, and furthermore we found that fusion was stimulated above the receptor-independent values by the high but not the low MHVR levels (data not shown). Thus, the S proteins of the prototype murine coronaviruses A59 and JHM were similar in that relatively high MHVR levels were necessary to enhance intercellular fusion.

(iii) The R^{lo} cells secrete high yields of progeny virus. We and others have found that abundant MHVR synthesis decreases the yields of infectious MHV-A59 particles (10, 30), but a complete mechanistic understanding of this inhibition is not yet available. To further investigate the role of MHVR levels during virus production, we monitored the time course of progeny virus development (Fig. 7). Interestingly, our findings indicated that the yields from both R^{lo} and R^{hi} cultures were similar up to 9 h postinfection, but after this time, yields from R^{lo} cells continued to increase while those from R^{hi} cells declined (Fig. 7A). We initially suspected the reduced virus production in R^{hi} cultures might be due to the cytopathology brought on by cell-cell fusion; by 8 h postinfection, R^{hi} cultures existed as a continuous macroscopic syncytium beginning to detach from its plastic substrate (Fig. 6A). However, this syncytium formation could not account for the low virus yields at the later time periods. Even in cultures seeded at densities low enough to prevent intercellular contact (10^4 cells per cm^2), similar time courses were observed. R^{hi} cells supported virus secretion to 9 h postinfection and then progressively lost this ability. R^{lo} cells continued to secrete increasing amounts of progeny to 15 h postinfection (Fig. 7B). These findings led us to speculate that virus infection of the R^{hi} cells, but not the R^{lo} cells, resulted in an acute single-cell death that was not dependent on the pathologic effects of syncytium formation.

(iv) The R^{hi} cells undergo an acute single-cell death following MHV-A59 infection. To investigate whether receptor levels affect the viabilities of infected cells, we inoculated subconfluent monolayers of R^{hi} and R^{lo} cells with MHV-A59 and then made two straightforward measurements. Viable cells were measured by trypan blue exclusion, and infected cells were measured by in situ immunostaining of the viral matrix protein. To ensure that any loss of cell viability was not due to syncytium formation, we added a fusion-blocking antiviral antiserum (MK15 rabbit antiserum) at 3 h postinfection. At the 1% concentration used, this antiserum blocked all fusion and additionally prevented superinfection by progeny virions (data not shown).

Our results revealed that the number of infected R^{hi} cells matched the number of cells that accepted the trypan blue dye

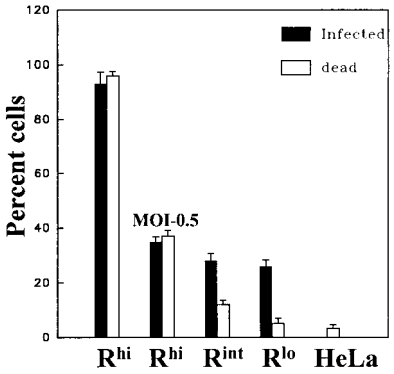

FIG. 8. Rapid virus-induced cell death in R^{hi} (but not R^{lo}) cells. Infection of subconfluent cells with MHV A59 (MOI = 100 PFU/cell) was followed 3 h later by addition of hyperimmune anti-A59 rabbit serum MK15 to 1% (final concentration). At 14 h postinfection, cells were suspended by using trypsin, and trypan blue was used to monitor cell lysis (white bars). Infected cells (black bars) were scored by indirect immunofluorescence as described in Materials and Methods. Error bars represent standard deviations from the average of four independent experiments.

(Fig. 8). This concordance between infected and nonviable R^{hi} cells remained even as the MOI was reduced to 0.5, indicating that the cell death was not due to the entry of an extraordinarily high number of virus particles. In contrast, the proportion of infected R^{int} and R^{lo} cells significantly exceeded the killed proportion. This indicated that individual cells can remain infected and viable for prolonged periods as long as the receptor levels remain relatively low. It must be noted, however, that these infected R^{lo} cells probably lack the capacity to replicate, as we have not been successful at establishing new cell colonies from individual infected R^{lo} cells.

(v) Ultrastructural analyses reveal a loss of organelle integrity in the infected R^{hi} cells. The infection process was rapidly cytotoxic only in the R^{hi} cells, and this toxicity was evident even in the absence of cell-to-cell contact. These findings prompted us to hypothesize that intracellular perturbations (i.e., formation of MHVR-S complexes within organelles) correlate with the rapid cell death. Thus, we set out to determine whether the presence of high MHVR levels during virus infection grossly affects intracellular architecture. We first used electron microscopic methods to visualize organelle integrity in the infected cells. Using this technique, we visualized vesicles loaded with virus particles (thin arrows) in both the R^{lo} and R^{hi} cells at 10 h postinfection (Fig. 9). However, only the R^{hi} cells showed obvious signs of necrosis. Cytoplasmic vacuoles and swelled, crista-damaged mitochondria were readily evident in the R^{hi} cells (thick arrows). There was no evidence of nuclear blebbing and chromatin condensation by this method (compare uninfected and infected sections), which suggested that the cell death we observed was not due to apoptosis (8, 39, 43).

Both MHVR and S proteins use the cellular exocytic pathway to reach the plasma membrane. This raised the possibility that S and MHVR might complex inside organelles of this pathway. In R^{hi} cells, such complexes might reach levels sufficient to disturb the structure and function of these organelles. To begin to address this hypothesis, we used immunofluorescence methods to localize the viral matrix protein within infected cells. We reasoned that matrix localization studies would help us to identify perturbations in this pathway, because matrix is produced abundantly, is normally retained in the Golgi (36), and does not interact directly with the MHVR. Thus, antimatrix antibody (12) was applied following fixation of R^{hi} or R^{lo} cells at various times postinfection, and this was followed by FITC immunostaining. Figure 10 depicts the fluorescence distribution at 12 h postinfection. In R^{lo} cells (Fig. 10B), the fluorescence was routinely clustered in a compact region that we contend corresponds to the Golgi apparatus, while fluorescence in R^{hi} cells (Fig. 10A) was dispersed throughout the cytoplasm in a diffuse array. Thus, abundant receptor production within A59-infected cells will impact matrix localization.

The viral spike protein will induce single-cell death in R^{hi} cells. Given that numerous findings implicate the MHV S protein in virus-induced cytopathology (14, 22) and given that the S protein is the only virus-encoded protein known to bind to MHVR (27), it was reasonable to suspect that acute cytolysis of R^{hi} cells would occur if S proteins were synthesized even in the absence of other coronavirus proteins. This possibility was addressed by constructing vaccinia virus vectors capable of producing the S proteins of various MHV strains and infecting R^{lo} or R^{hi} cells with these vectors.

Cytolysis was measured by the trypan blue exclusion method at 12 h after vaccinia virus infection. To ensure that our assays measured cytolysis of single cells, we prevented the possibility of multinucleated syncytia through the use of subconfluent cells and the fusion-blocking antiviral rabbit serum MK15, as described above. Our results (Fig. 11) revealed that the S protein of strain JHM (S_{JHM}) was powerfully cytopathic (60% trypan blue-positive cells) in R^{hi} cells but was 10-fold less potent in this regard in the R^{lo} cells. The complete, membrane-anchored S_{JHM} was required to mediate this cytopathic effect, as production of either the soluble ectodomain form of S or the receptor-binding S1 posttranslation fragment (52) failed to render R^{hi} cells permeable to trypan blue. Since the membrane fusion potential of S proteins requires that they exist in a membrane-anchored form (57), we suspected that fusion activities might be involved in cytopathology. This was further addressed by synthesizing the S proteins of two other MHV strains from vaccinia virus vectors, OBL and A59 (32, 55). We measured the relative capacities of these two S proteins to induce intercellular fusion using the cytoplasmic content mixing assay, as previously described (45, 46). We found that the fusion potentials of S_{OBL} and S_{A59} were one-third and one-fourth that of S_{JHM}, respectively. Furthermore we found that S_{OBL} and S_{A59} proteins were about one-half as effective as S_{JHM} in the cytolysis of R^{hi} cells (Fig. 11), suggesting that a direct relationship exists between the fusion potential of the S protein and its cytopathic effect on single, well-separated cells.

Spike and receptor proteins form intracellular complexes. Our findings on the effect of the S protein on R^{lo} and R^{hi} cell viability suggested to us that cytolysis results from the accumulation of S-MHVR complexes within intracellular compartments. Thus, we set out to identify such complexes by examining whether antireceptor antibodies might coimmunoprecipitate both the MHVR and S proteins. This approach was tenable because we had access to a monospecific antipeptide antibody (R874) directed against the carboxy-terminal 16 amino acids of the MHVR that we had previously determined to be effective and specific in its ability to immunoprecipitate the receptor (46). Because this antibody recognized an epitope that was distant from the portion of the MHVR that binds to S (20), we reasoned that it would be exposed on both free MHVR and MHVR that was associated with the S protein.

To determine whether the R^{hi} or R^{lo} cells that also produce S_{JHM} protein contain S-MHVR complexes, we radiolabeled the cells producing S_{JHM} with [^{35}S]methionine prior to NP-40-mediated lysis and immunoprecipitation with the antireceptor antibody. ^{35}S-labeled proteins of sizes consistent with the MHVR (110 kDa) and the uncleaved S_{JHM} precursor (180 kDa) were indeed identified in electrophoretic profiles of the ^{35}S-labeled proteins precipitated from R^{hi} cells (Fig. 12A, lanes 1 and 2, respectively). As expected, equivalent numbers of R^{lo} cells that were analyzed in parallel contained markedly lower amounts of the ^{35}S-labeled S-MHVR complexes (Fig. 12A, lane 4).

To determine whether the MHVR had complexed with intracellular form(s) of the uncleaved S_{JHM} precursor, we treated the precipitated ^{35}S-labeled S-MHVR complexes with endoglycosidase H prior to electrophoresis. The endoglycosidase H exposure decreased the apparent molecular weight of the S protein by ~30 kDa (Fig. 12A, lane 3). This indicated that the uncleaved S proteins that were complexed with the MHVR had failed to reach a Golgi complex capable of converting N-linked carbohydrates to an endoglycosidase H-resistant form. Similar findings were obtained when the S proteins that were synthesized in the R^{hi} cells were soluble S_{ecto} molecules (Fig. 12A, lanes 5 and 6). From these results, we speculate that complexes of MHVR and S, once formed in premedial Golgi compartments, fail to acquire competence for continued transport through the exocytic pathway.

We suspected that the expression of S_{JHM} cDNA from our vaccinia virus vectors would produce more than 300,000 S

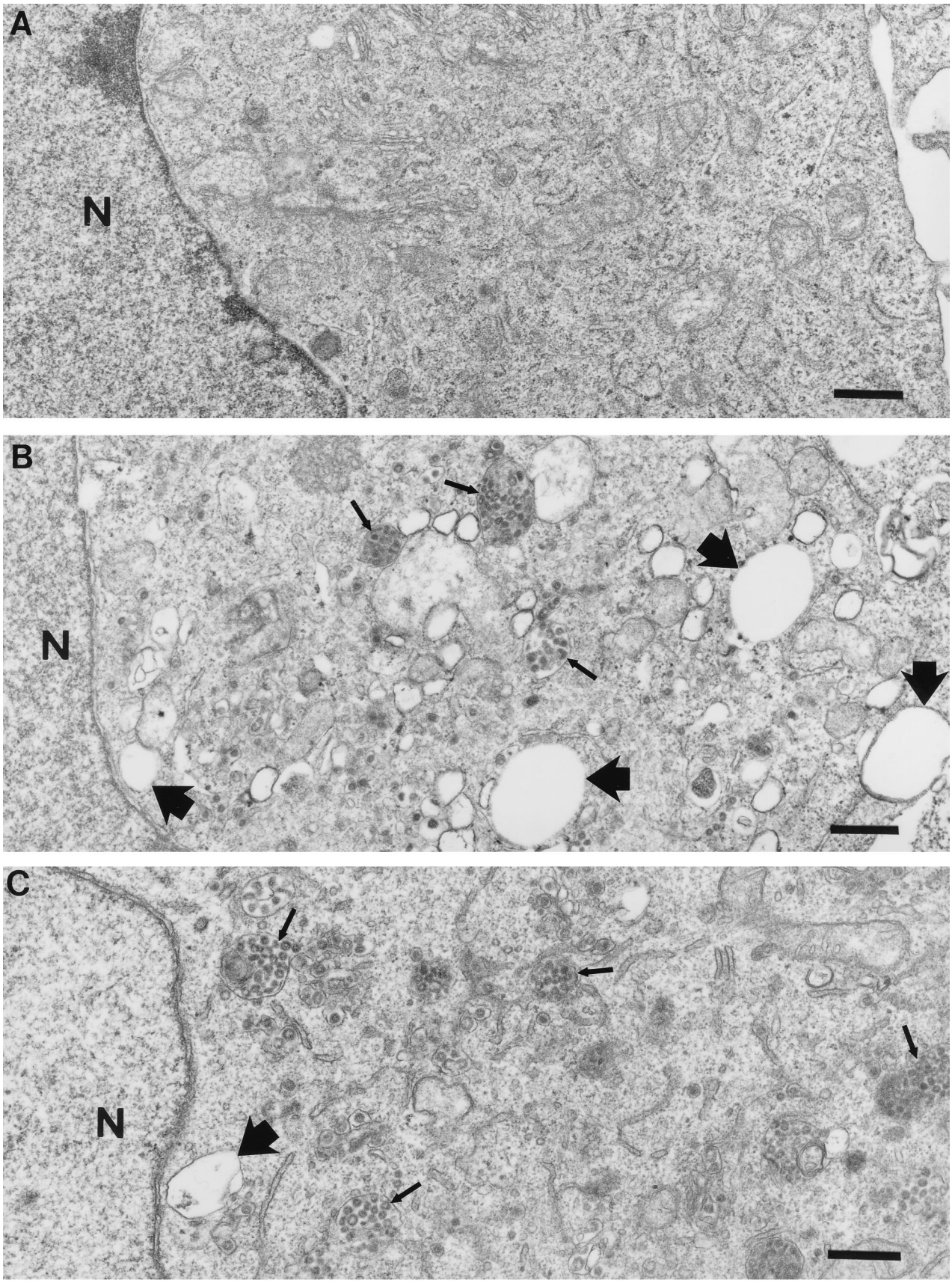

FIG. 9. Transmission electron micrographs of MHV-A59-infected HeLa-MHVR cells. Cells were processed for microscopy at 10 h postinfection (MOI = 10 PFU/cell). Thin arrows point to virus-containing vesicles; thick arrows point to vacuoles. N, nucleus. (A) Mock-infected R^{hi}; (B) A59-infected R^{hi}; (C) A59-infected R^{lo}. Bars represent 0.5 μm.

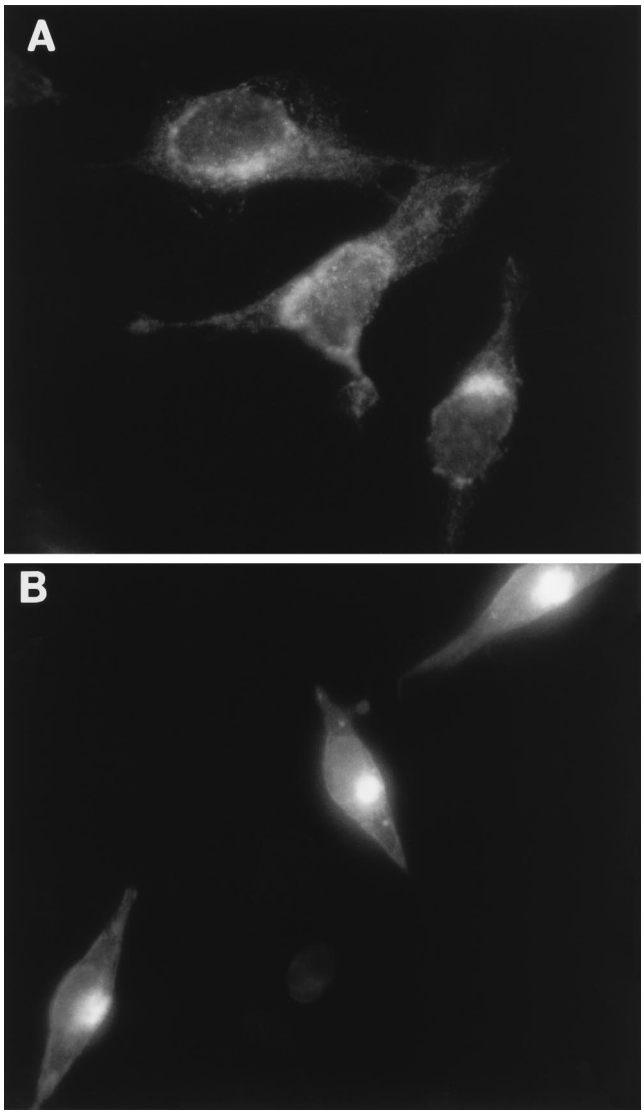

FIG. 10. Distribution of the viral matrix protein in MHV A59-infected HeLa-MHVR cells. Subconfluent monolayers were processed for indirect immunofluorescence at 12 h postinfection (MOI = 100 PFU/cell) and photographed with a Leitz fluorescence microscope. Exposure times were identical. (A) R^{hi}; (B) R^{lo}.

proteins per cell (25) and therefore would exceed the number of receptors produced in R^{hi} cells. If this were indeed the case, then all receptor molecules in the R^{hi} cultures might be complexed with the endogenously synthesized S proteins, and consequently would be unavailable for interaction with exogenously added ^{35}S-virions. We addressed this question by adding purified ^{35}S-MHV-A59 to cultures of R^{hi} cells that had been infected 12 h earlier with the S-expressing vaccinia vectors. We then immediately lysed the cells along with the associated ^{35}S-virions by using NP-40 detergent and then immunoprecipitated the MHVR proteins with antireceptor antibody.

Electrophoretic analyses of the radioactive proteins that coprecipitated with the unlabeled MHVR (Fig. 12B) revealed that the MHVR from the R^{hi} cells was indeed capable of binding the exogenously added radioactive A59 S proteins (lane 7). In contrast, the same amount of MHVR from the cultures synthesizing the S_{JHM} was entirely unable to precipitate the radioactive S protein (lane 8). However, this radioactive S protein was partially recovered from the same cell lysate by precipitation with 100 ng of soluble recombinant MHVR (28), as depicted in lane 9. Thus we conclude that the MHVR proteins in S-producing cells were fully occupied by the endogenously synthesized JHM S molecules before the cell lysis was performed.

DISCUSSION

MHV infections exhibit remarkable variability in cytopathology, ranging from acutely cytolytic to essentially asymptomatic levels in cultured cells (13, 42). This range of MHV-induced cytopathology has generally been considered to be dependent on the variable activity of the S protein. S proteins can induce a cytotoxic intercellular membrane fusion, the potency of which depends on numerous factors including the capacity of newly synthesized S proteins to fold, assemble, and transport to the cell surface, the susceptibility of S to proteolytic cleavage by host cell proteases (23), the lipid composition of the host cell (9, 47), and the pH of the extracellular environment (48). This study has identified the receptor to which S proteins bind (the MHVR) as yet another determinant of MHV-induced cytopathology. In fact, in our system involving HeLa-MHVR transfectant cell lines as hosts for MHV infection, the level of receptor production was the primary determinant of virus-induced cytopathology. In our system, the synthesis and processing of the S protein—indeed, the entire productive infection process—was not in and of itself powerfully cytotoxic. Rather, it was the concomitant synthesis of two proteins, S and MHVR, that accounted for the virus-induced death of the HeLa-MHVR cells.

Regulated production of the MHVR in HeLa-MHVR transfectants allowed us to determine that the amount of cell surface MHVR required for infection by incoming virions was lower than that required to promote membrane fusion between infected cells. Thus, R^{lo} cells could be infected and could support development of progeny virions for prolonged

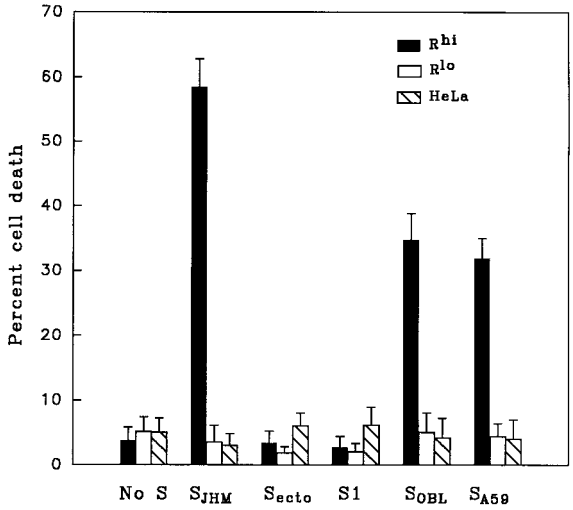

FIG. 11. Measurement of single-cell death induced by production of the MHV S protein. Subconfluent densities of HeLa-MHVR cells were coinfected with vTF7.3 along with the indicated vTM1-based recombinants encoding various forms of the MHV spike (S_{JHM}, S_{ecto}, S1, S_{OBL}, and S_{A59}). At 3 h postinfection, the fusion inhibiting antibody MK15 was added. Cells were trypsinized at 12 h postinfection, and the number of viable cells was determined by trypan blue exclusion. Error bars represent standard deviations from the mean obtained from six independent experiments.

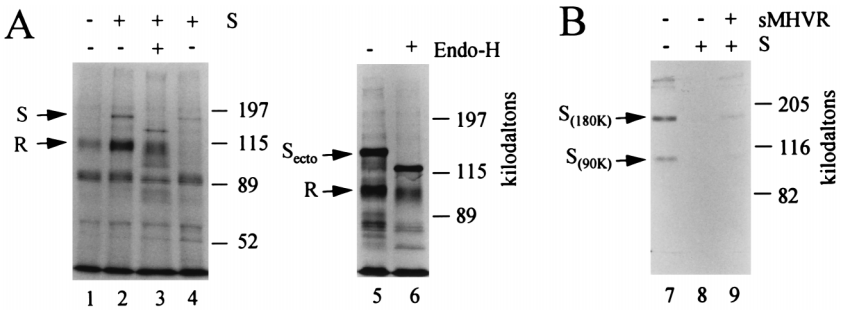

FIG. 12. Coimmunoprecipitation of MHVR and S from cells producing both proteins. (A) R^{hi} or R^{lo} cells were coinfected with vaccinia virus recombinants vTF7.3 and vTM1-S_{JHM} and then radiolabeled with Tran[^{35}S]-label from 3 to 7 h postinfection. Immediately after labeling, cytoplasmic extracts were prepared by the NP-40 lysis procedure, and ^{35}S-labeled proteins were immunoprecipitated with antireceptor antiserum and Sepharose-protein G. Proteins bound to the Sepharose-protein G were treated with endoglycosidase H (+) or left untreated (−) and then prepared for SDS-polyacrylamide gel electrophoresis. The separated proteins were visualized by fluorography. Lane 1, R^{hi} cells (vTF7.3 plus VVWR) (control; no S produced); lanes 2 and 3, R^{hi} cells (vTF7.3 plus vTM1-S_{JHM}); lane 4, R^{lo} cells (vTF7.3 plus vTM1-S_{JHM}); lanes 5 and 6, R^{hi} cells (vTF7.3 plus vTM1-S_{ecto}. (B) R^{hi} cells were coinfected with vTF7.3 and vTM1-S_{JHM}. At 12 h postinfection, cells were lysed along with exogenously added ^{35}S-labeled A59 virions (12×10^4 cpm) and then immunoprecipitated with antireceptor antibody as described above. Precipitations were performed in the absence or presence of exogenously added sMHVR, which specifically absorbs S proteins to Sepharose-protein G (28). Immunoprecipitates were subjected to SDS-polyacrylamide gel electrophoresis and fluorography. Lane 7, vTF7.3 plus VVWR; lanes 8 and 9, vTF7.3 plus vTM1-S_{JHM}.

periods without suffering from the toxic effects accompanying syncytium formation. This finding that virions, but not infected cells, could successfully fuse with the R^{lo} cells suggested that the two membrane fusion events have unique requirements. Distinct requirements were actually considered likely, as previous studies of retro- and paramyxoviruses have shown that the virion-cell fusion process can readily occur under conditions in which the cognate cell-cell fusion is limited. Virion-cell fusion can occur at low temperature (3), in the presence of syncytium-blocking peptides (38), and at relatively low receptor levels (4, 50). Hints that the virion-cell fusion during coronavirus infection might similarly occur more readily than the corresponding cell-cell fusion is suggested by its exclusive occurrence even when viral S proteins remain largely as relatively inactive, uncleaved S precursors (33). To explain our observation of successful virion-cell fusion at low MHVR levels, we suggest that S proteins must be closely spaced for fusion to occur and that such close spacing is found on the virion surface but not the infected cell surface. We further hypothesize that MHVR levels must be relatively high to congregate the S proteins found on the infected cell surface into the close proximities necessary to promote fusion. Such a hypothesis would be consistent with previous findings indicating that virus-induced membrane fusion requires the formation of arrays of nearby viral glycoproteins (15, 24, 57).

We initially thought that the cytotoxicity arising from abundant MHVR levels was due solely to its role in promoting the intercellular fusion events that ultimately produce syncytia (i.e., Fig. 6). Thus, we were surprised to find that our R^{hi} cells died within ~14 h following infection even when separated from each other (Fig. 8). We obtained similar results when we infected the HeLa-MHVR cells with vaccinia virus-S recombinants (Fig. 11). This led us to conclude that the abundance of MHVR strongly influenced the cytotoxicity of endogenously synthesized S proteins by mechanism(s) that were independent of syncytium formation.

Numerous findings lead us to suggest that the coexpression of S and MHVR in cells could generate cytotoxic, intracytoplasmic membrane fusion events. First, only complete, membrane-anchored forms of S were able to cause the death of individual, well-separated R^{hi} cells (Fig. 11). Soluble S ectodomain fragments that cannot induce membrane fusion (S1 or the complete S1/S2 ectodomain) were far less cytotoxic, even though they bound avidly to the MHVR within the cell (Fig. 12). Second, complete S proteins that were identical to those produced by the weakly fusogenic MHV strains A59 and OBL (31, 32) were less cytotoxic than the corresponding highly fusogenic JHM S proteins (Fig. 11), indicating that toxicity and fusion potentials are correlated. Third, the intracellular architecture in cells producing both MHVR and S in abundance was clearly distinct from those cells in which lower amounts of MHVR were produced (Fig. 9 and 10); this raises the possibility of fusion between or within intracellular vesicles. Finally, we were able to specifically immunoprecipitate complexes of S and MHVR from infected R^{hi} lysates, and we could document their predominance in premedial Golgi locations (Fig. 12). Thus, we hypothesize that the accumulation of these complexes impairs intracellular integrity of organelles and ultimately causes necrosis and cell death.

In contrast to the R^{hi} cells, our R^{lo} cells survive MHV infection without ever undergoing any acute cytolytic phase, and they continuously secrete high titers of progeny (Fig. 7 and data not shown). Notably, we found that our infected R^{hi} cells would similarly develop into persistently infected cultures, but only after an acute phase of infection that destroyed all but the few cells (<1%) producing low levels of MHVR; i.e., cells repopulating the cultures were R^{lo} (data not shown). Thus, the maintenance of persistent infection requires establishment of cultures in which MHVR levels are low. This important finding has been previously documented in studies of persistently infected murine cell cultures (11, 48).

Is it possible that the relative levels of MHVR in vivo might help to explain the nature of MHV-induced cytopathologies? One might speculate that such is the case given what is currently known about in vivo MHVR levels and their relationship to sites of persistent virus infection. MHVR levels in the murine central nervous system are substantially lower than those found in peripheral organs such as the liver and intestine (58, 59), and persistent virus infection is generally restricted to the central nervous system. These findings justify consideration of MHVR levels as one of many factors determining the pathology of in vivo infection. Since the tetracycline-controlled system used in our studies is adaptable to the in vivo environment (5, 34), this interesting question may soon be addressed through experimentation.

ACKNOWLEDGMENTS

We thank Bonnie Hsiang and Erica Sethi for assistance in developing and maintaining the HeLa-MHVR cell lines. We also thank Hans-Martin Jäck, H. Gössen, and J. Bujard for providing the HeLa-tTA cells and the pUHD-10-3 expression vector. Special thanks go to Kathryn V. Holmes and Michael J. Buchmeier for their precious gifts of antireceptor antibodies CC1 and R874, respectively. We are indebted to John McNulty and Linda Fox for assistance with electron microscopy and to Tom Ellis and Patricia Simms for assistance with FACS.

This research was supported by NIH grant NS31636 and by a grant from the Schweppe Foundation of Chicago.

REFERENCES

1. **Ahmed, R., L. A. Morrison, and D. M. Knipe.** 1996. Persistence of viruses, p. 219–249. *In* B. N. Fields, D. M. Knipe, and P. M. Howley (ed.), Fields virology, vol. 1, 3rd ed. Lippincott-Raven, New York, N.Y.
2. **Alexander, W. A., B. Moss, and T. R. Fuerst.** 1992. Regulated expression of foreign genes in vaccinia virus under the control of bacteriophage T7 RNA polymerase and the *Escherichia coli lac* repressor. J. Virol. **66:**2934–2942.
3. **Aroeti, B., and Y. I. Henis.** 1988. Effects of fusion temperature on the lateral mobility of sendai virus glycoproteins in erythrocyte membranes and on cell fusion indicate that glycoprotein mobilization is required for cell fusion. Biochemistry **27:**5654–5661.
4. **Asjö, B., I. Ivhed, M. Gidlund, S. Fuerstenberg, E. M. Fenyö, K. Nilsson, and H. Wigzell.** 1987. Susceptibility to infection by the human immunodeficiency virus (HIV) correlates with T4 expression in a parental monocytoid cell lines and its subclones. Virology **157:**359–365.
5. **Baron, U., M. Gossen, and H. Bujard.** 1997. Tetracycline-controlled transcription in eukaryotes: novel transactivators with graded transactivation potential. Nucleic Acids Res. **25:**2723–2729.
6. **Baybutt, H. N., H. Wege, M. J. Carter, and V. Ter Meulen.** 1984. Adaptation of coronavirus JHM to persistent infection of murine Sac (−) cells. J. Gen. Virol. **65:**915–924.
7. **Buchmeier, M. J., R. M. Welsh, F. J. Dutko, and M. B. A. Oldstone.** 1980. The virology and immunology of lymphocytic choriomeningitis virus infection. Adv. Immunol. **30:**275–331.
8. **Cao, J., I.-W. Park, A. Cooper, and J. Sodroski.** 1996. Molecular determinants of acute single-cell lysis by human immunodeficiency virus type 1. J. Virol. **70:**1340–1354.
9. **Cervin, M., and R. Anderson.** 1991. Modulation of coronavirus-mediated cell fusion by homeostatic control of cholesterol and fatty acid metabolism. J. Med. Virol. **35:**142–149.
10. **Chen, W., V. J. Madden, C. R. Bagnell, Jr., and R. S. Baric.** 1997. Host-derived intracellular immunization against mouse hepatitis virus infection. Virology **228:**318–332.
11. **Chen, W., and R. S. Baric.** 1996. Molecular anatomy of mouse hepatitis virus persistence: coevolution of increased host cell resistance and virus virulence. J. Virol. **70:**3947–3960.
12. **Collins, A. R., R. L. Knobler, H. Powell, and M. J. Buchmeier.** 1982. Monoclonal antibodies to murine hepatitis virus-4 (strain JHM) define the viral glycoprotein responsible for attachment and cell-cell fusion. Virology **119:**358–371.
13. **Dales, S., and R. Anderson.** 1995. Pathogenesis and diseases of the central nervous system caused by murine coronaviruses, p. 257–292. *In* S. G. Siddell (ed.), The Coronaviridae. Plenum Press, New York, N.Y.
14. **Dalziel, R. G., P. W. Lampert, P. J. Talbot, and M. J. Buchmeier.** 1986. Site-specific alteration of murine hepatitis virus type 4 peplomer glycoprotein E2 results in reduced neurovirulence. J. Virol. **59:**463–471.
15. **Danieli, T., S. L. Pelletier, Y. I. Henis, and J. M. White.** 1996. Membrane fusion mediated by influenza virus hemagglutinin requires the concerted action of at least three hemagglutinin trimers. J. Cell Biol. **133:**559–569.
16. **Davies, H. A., and M. R. Macnaughton.** 1979. Comparison of the morphology of three coronaviruses. Arch. Virol. **59:**25–33.
17. **Daya, M., M. Cervin, and R. Anderson.** 1988. Cholesterol enhances mouse hepatitis virus-mediated cell fusion. Virology **163:**276–283.
18. **Dermody, T. S., M. L. Nibert, J. D. Wetzel, X. Tong, and B. N. Fields.** 1993. Cells and viruses with mutations affecting viral entry are selected during persistent infections of L cells with mammalian reoviruses. J. Virol. **67:**2055–2063.
19. **Dveksler, G. S., A. A. Basile, C. B. Cardellichio, and K. V. Holmes.** 1995. Mouse hepatitis virus receptor activities of an MHVR/mph chimera and MHVR mutants lacking N-linked glycosylation of the N-terminal domain. J. Virol. **69:**543–546.
20. **Dveksler, G. S., M. N. Pensiero, C. W. Dieffenbach, C. B. Cardellichio, A. A. Basile, P. E. Elia, and K. V. Holmes.** 1993. Mouse hepatitis virus strain A59 and blocking antireceptor monoclonal antibody bind to the N-terminal domain of cellular receptor. Proc. Natl. Acad. Sci. USA **90:**1716–1720.
21. **Dveksler, G. S., M. N. Pensiero, C. B. Cardellichio, R. K. Williams, G.-S. Jiang, K. V. Holmes, and C. W. Dieffenbach.** 1991. Cloning of the mouse hepatitis virus (MHV) receptor: expression in human and hamster cell lines confers susceptibility to MHV. J. Virol. **65:**6881–6891.
22. **Fazakerley, J. K., S. E. Parker, F. Bloom, and M. J. Buchmeier.** 1992. The V5A13.1 envelope glycoprotein deletion mutant of mouse hepatitis virus type-4 is neuroattenuated by its reduced rate of spread in the central nervous system. Virology **187:**178–188.
23. **Frana, M. F., J. N. Behnke, L. S. Sturman, and K. V. Holmes.** 1985. Proteolytic cleavage of the E2 glycoprotein of murine coronavirus:host-dependent differences in proteolytic cleavage and cell fusion. J. Virol. **56:**912–920.
24. **Frey, S., M. Marsh, S. Günther, A. Pelchen-Matthews, P. Stephens, S. Ortlepp, and T. Stegmann.** 1995. Temperature dependence of cell-cell fusion induced by the envelope glycoprotein of human immunodeficiency virus type 1. J. Virol. **69:**1462–1472.
25. **Fuerst, T. R., P. L. Earl, and B. Moss.** 1987. Use of a hybrid vaccinia virus-T7 RNA polymerase system for expression of target genes. Mol. Cell. Biol. **7:**2538–2544.
26. **Fuerst, T. R., E. G. Niles, F. W. Studier, and B. Moss.** 1986. Eukaryotic transient expression system based on recombinant vaccinia virus that synthesizes bacteriophage T7 RNA polymerase. Proc. Natl. Acad. Sci. USA **83:**8122–8126.
27. **Gagneten, S., O. Gout, M. Dubois-Dalcq, P. Rottier, J. Rossen, and K. V. Holmes.** 1995. Interaction of mouse hepatitis virus (MHV) spike glycoprotein with receptor glycoprotein MHVR is required for infection with an MHV strain that expresses the hemagglutinin-esterase glycoprotein. J. Virol. **69:**889–895.
28. **Gallagher, T. M.** 1997. A role for naturally occurring variation of the murine coronavirus spike protein in stabilizing association with the cellular receptor. J. Virol. **71:**3129–3137.
29. **Gallagher, T. M.** 1996. Murine coronavirus membrane fusion is blocked by modification of thiols buried within the spike protein. J. Virol. **70:**4683–4690.
30. **Gallagher, T. M.** 1995. Overexpression of the MHV receptor: effect on progeny virus secretion. Adv. Exp. Med. Biol. **380:**331–336.
31. **Gallagher, T. M., M. J. Buchmeier, and S. Perlman.** 1992. Cell receptor-independent infection by a neurotropic murine coronavirus. Virology **191:**517–522.
32. **Gallagher, T. M., C. Escarmis, and M. J. Buchmeier.** 1991. Alteration of the pH dependence of coronavirus-induced cell fusion: effect of mutations in the spike glycoprotein. J. Virol. **65:**1916–1928.
33. **Gombold, J. L., S. T. Hingley, and S. R. Weiss.** 1993. Fusion-defective mutants of mouse hepatitis virus A59 contain a mutation in the spike protein cleavage signal. J. Virol. **67:**4504–4512.
34. **Gossen, M., S. Freundlieb, G. Bender, G. Müller, W. Hillen, and H. Bujard.** 1995. Transcriptional activation by tetracyclines in mammalian cells. Science **268:**1766–1769.
35. **Gossen, M., and H. Bujard.** 1992. Tight control of gene expression in mammalian cells by tetracycline-responsive promoters. Proc. Natl. Acad. Sci. USA **89:**5547–5551.
36. **Klumperman, J., J. K. Locker, A. Meijer, M. C. Horzinek, H. J. Geuze, and P. J. M. Rottier.** 1994. Coronavirus M proteins accumulate in the golgi complex beyond the site of virion budding. J. Virol. **68:**6523–6534.
37. **Knobler, R. L., P. W. Lampert, and M. B. A. Oldstone.** 1982. Virus persistence and recurring demyelination produced by a temperature-sensitive mutant of MHV-4. Nature **298:**279–280.
38. **Konopka, K., E. Pretzer, and N. Duzgunes.** 1995. Differential effects of a hydrophobic tripeptide on human immunodeficiency virus type 1 (HIV-1)-induced syncytium formation and viral infectivity. Biochem. Biophys. Res. Commun. **208:**75–81.
39. **Koolen, M. J. M., S. Love, W. Wouda, J. Calafat, M. C. Horzinek, and B. A. M. Van Der Zeijst.** 1987. Induction of demyelination by a temperature-sensitive mutant of the coronavirus MHV-A59 is associated with restriction of viral replication in the brain. J. Gen. Virol. **68:**703–714.
40. **Laemmli, U. K.** 1970. Cleavage of structural proteins during the assembly of the head of bacteriophage T4. Nature **227:**680–685.
41. **Lai, M. M. C.** 1990. Coronavirus: organization, replication and expression of genome. Annu. Rev. Microbiol. **44:**303–333.
42. **Lavi, E., A. Suzumura, M. Hiragama, M. K. Highkin, D. M. Dambach, D. H. Silberberg, and S. R. Weiss.** 1987. Coronavirus mouse hepatitis virus (MHV)-A59 causes persistent, productive infection in primary glial cell cultures. Microb. Pathol. **3:**79.
43. **Majno, G., and I. Joris.** 1995. Apoptosis, oncosis and necrosis, an overview of cell death. Am. J. Pathol. **146:**3–15.
44. **Nash, T. C., and M. J. Buchmeier.** 1996. Spike glycoprotein-mediated fusion in biliary glycoprotein-independent cell-associated spread of mouse hepatitis virus infection. Virology **223:**68–78.
45. **Nussbaum, O., C. C. Broder, and E. A. Berger.** 1994. Fusogenic mechanisms of enveloped-virus glycoproteins analyzed by a novel recombinant vaccinia virus-based assay quantitating cell fusion-dependent reporter gene activation. J. Virol. **68:**5411–5422.
46. **Rao, P. V., S. Kumari, and T. M. Gallagher.** 1997. Identification of a contiguous 6-residue determinant in the MHV receptor that controls the level of virion binding to cells. Virology **229:**336–348.
47. **Roos, D. S., C. S. Duchala, C. B. Stephensen, K. V. Holmes, and P. W.**

Choppin. 1990. Control of virus-induced cell fusion by host cell lipid composition. Virology **175:**345–357.
48. **Sawicki, S. G., J.-H. Lu, and K. V. Holmes.** 1995. Persistent infection of cultured cells with mouse hepatitis virus (MHV) results from the epigenetic expression of the MHV receptor. J. Virol. **69:**5535–5543.
49. **Stohlman, S. A., A. Y. Sakaguchi, and L. P. Weiner.** 1979. Characterization of the cold-sensitive murine hepatitis virus mutants rescued from latently infected cells by cell fusion. Virology **98:**448–455.
50. **Siess, D. C., S. L. Kozak, and D. Kabat.** 1996. Exceptional fusogenicity of Chinese hamster ovary cells with murine retroviruses suggests roles for cellular factor(s) and receptor clusters in the membrane fusion process. J. Virol. **70:**3432–3439.
51. **Sturman, L. S., and K. K. Takemoto.** 1972. Enhanced growth of a murine coronavirus in transformed mouse cells. Infect. Immun. **6:**501–507.
52. **Suzuki, H., and F. Taguchi.** 1996. Analysis of the receptor-binding site of murine coronavirus spike protein. J. Virol. **70:**2632–2636.
53. **Taguchi, F.** 1993. Fusion formation by the uncleaved spike protein of murine coronavirus JHMV variant cl-2. J. Virol. **67:**1195–1202.
54. **Taguchi, F., and S. G. Siddell.** 1985. Differences in sensitivity to interferon among mouse hepatitis viruses with high and low virulence for mice. Virology **147:**41–48.
55. **Vennema, H., L. Heijnen, A. Zijderveld, M. C. Horzinek, and W. J. M. Spaan.** 1990. Intracellular transport of recombinant coronavirus spike proteins: implications for virus assembly. J. Virol. **64:**339–346.
56. **Wang, F.-L., J. O. Fleming, and M. M. C. Lai.** 1992. Sequence analysis of the spike protein gene of murine coronavirus variants: study of genetic sites affecting neuropathogenicity. Virology **186:**742–749.
57. **White, J. M.** 1992. Membrane fusion. Science **258:**917–924.
58. **Williams, R. K., G.-S. Jiang, S. W. Snyder, M. F. Frana, and K. V. Holmes.** 1990. Purification of the 110-kilodalton glycoprotein receptor for mouse hepatitis virus (MHV)-A59 from mouse liver and identification of a nonfunctional, homologous protein in MHV-resistant SJL/J mice. J. Virol. **64:**3817–3823.
59. **Yokomori, K., and M. M. C. Lai.** 1992. Mouse hepatitis virus utilizes two carcinoembryonic antigens as alternative receptors. J. Virol. **66:**6194–6199.